

55

B12, B25

TK 36.889

KFKI-71-11



I. Kósa Somogyi

ELECTRICAL CONDUCTIVITY OF IRRADIATED  
DIELECTRIC ORGANIC LIQUIDS AND GLASSES

*Hungarian Academy of Sciences*

CENTRAL  
RESEARCH  
INSTITUTE FOR  
PHYSICS

BUDAPEST



KFKI-71-11

**ELECTRICAL CONDUCTIVITY OF IRRADIATED DIELECTRIC ORGANIC  
LIQUIDS AND GLASSES**

**I. Kósa Somogyi**

**Central Research Institute for Physics, Budapest/Hungary/  
Nuclear Chemistry Department**

## ABSTRACT

Recent investigations concerning electrical conduction in dielectric liquids and glasses are reviewed. The relationship between the free ion yield and the increase in the electrical current on irradiation is discussed with special regard to the role of recombination processes, viscosity, pressure and the dielectric constant of the system. The predictions of the most advanced theoretical models are compared with the experimental data. The methods of measuring current, charge carrier mobility and lifetime are briefly described and attention is drawn to the possible influence of the nature of the electrodes and the effects of space charge and potential variations during the irradiation of glasses and dielectric organic liquids. The current peaks observed during the warming of glasses irradiated at low temperature are explained in terms of structural changes and electret formation. The values of  $G_{fi}$  calculated for different organic liquids from the measured conduction are tabulated with the parameters used in calculation.

## РЕЗЮМЕ

В обзоре рассмотрены исследования по электропроводности облученных диэлектрических жидкостей и стекол. Показана зависимость между увеличением тока и выходом "свободных" ионов, обсуждена роль рекомбинации, давления и диэлектрической постоянной в изученных системах. Предсказания некоторых теоретических моделей сравниваются с экспериментальными данными. Описаны методы измерения малых токов подвижности и времени жизни носителей зарядов, сделана попытка объяснения на происходящие процессы возможного влияния свойств электродов, поля пространственного заряда и изменения потенциала во время облучения органических жидких диэлектриков и стекол. Пики термостимулированного тока облученных при низких температурах органических стекол связываются с изменениями структуры и с образованием электретов. Радиационно-химические выходы "свободных" ионов  $G_{fi}$  вычисленные по измеренным токам, и некоторые параметры, использованные при вычислениях для ряда веществ, даются в прилагаемой таблице.

## KIVONAT

A cikk áttekintést ad a szigetelő folyadékok és üvegek elektromos vezetőképességére vonatkozó újabb kutatásokról. A szabad ionok hozama és a besugárzás okozta áramnövekedés közötti összefüggést ismerteti, különös tekintettel a rekombinációs folyamatoknak, a viszkozitásnak, a nyomásnak és az anyagok dielektromos állandójának szerepére. A legújabb elméleti modellek alapján végzett számítások eredményeit hasonlítja össze a kísérleti adatokkal. Az áram, töltéshordozó mozgékonyság és élettartam mérések módszereinek rövid ismertetésénél felhívja a figyelmet az alkalmazott elektródák típusának, a besugárzás alatti tértöltés- és potenciálváltozásoknak esetleges, de még nem eléggé tisztázott befolyására. Az alacsony hőmérsékleten besugárzott üvegek felmelegedésekor megfigyelt hirtelen áramnövekedéseket szerkezeti átalakulásokkal és elektret képződéssel magyarázza. A különböző szerves folyadékokon mért vezetőképességből számított  $G_{fi}$  értékeket és a számításokhoz használt paramétereket táblázatos formában közli.

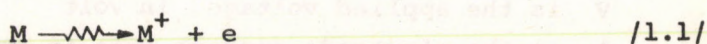
	Page
1. INTRODUCTION	1
1.1. Relationship between $G_{fi}$ and the measured current	1
1.2. The effect of viscosity and pressure on $G_{fi}$	3
2. EVALUATION OF THE FREE ION YIELD $G_{fi}$	4
2.1. Range-energy relation for electrons	4
2.2. The time dependence of $G_{fi}$	8
3. METHODOLOGY	12
3.1. Measurement of steady state current	12
3.2. Mobility measurements	14
3.3. Charge carrier lifetime	16
4. FACTORS OTHER THAN RADIATION AFFECTING THE CONDUCTIVITY	17
4.1. The role of electrodes	17
4.2. Potential distribution within the conductivity cell	21
4.3. Current peaks during warmup	26
5. COMPILATION OF THE REPORTED DATA	29
6. CONCLUDING REMARKS	29
7. REFERENCES	34



## 1. INTRODUCTION

### 1.1. Relationship between $G_{fi}$ and the measured current, $i$

On the exposure of matter to high energy radiation ionization takes place in the form



where  $M^+$  is the positive molecular ion and  $e^-$  is the electron. The ejected electrons have a wide spread of energy. The energetic ions are capable of inducing further ionization during their thermalization, thus giving birth to secondary, tertiary, etc. electrons in the irradiated system. In liquids usually more than 90 percent of these electrons are neutralized within about  $10^{-11}$  sec by recombination with their parent ions or with ions in the same spur [1], and only a minor fraction can escape from the attractive field of the ions. Electrons that do escape become thermalized at a distance from their parent ions at which the thermal energy is higher than the coulombic attraction energy. Until they finally encounter a positive ion, these electrons are free to diffuse at random in the system. The time taken by this diffusion is many orders longer than the recombination time, and in some favourable cases it may be of the order of seconds. The diffusion of the escaped /or quasi-free/ electrons can be oriented and enhanced by the presence of an external electric field. Thus, an applied field permits the observation of an increase in the electric current in the irradiated sample. Eventually all the quasi-free electrons are neutralized by positive ions crossing their path, so that under continuous irradiation a steady state sets in when the rate of formation of charge carriers equals their rate of recombination. The steady state can be described by the formula

$$\frac{dn}{dt} = F - k'n^2 = 0 \quad /1.2/$$

where  $n$  is the number of escaped electrons / = number of positive ions / per  $\text{cm}^3$ ;  $F$  is the rate of electron escape / =  $10^{-2} \dot{D} G_{fi}$  /;  $\dot{D}$  is the dose rate, in  $\text{eV cm}^{-3} \text{sec}^{-1}$ ; and  $k'$  is the ion neutralization rate constant, in  $\text{cm}^3 \text{sec}^{-1}$ . The free ion yield, in ions per 100 eV, is given by

$$G_{fi} = \frac{k'e^2 n^2}{10^{-2} \dot{D}} = \frac{100 k'}{\mu} \frac{\sigma^2}{\mu \dot{D}} \quad /1.3/$$

since

$$\sigma = ne\mu = \frac{iL}{VA}, \quad /1.4/$$

where  $\sigma$  is the conductivity in  $\text{ohm}^{-1}\text{cm}^{-1}$   
 $\mu$  is the mobility of the charge carriers, in  $\text{cm}^2\text{volt}^{-1}\text{sec}^{-1}$   
 $i$  is the current, in amp  
 $L$  is the distance between the electrodes, in cm  
 $V$  is the applied voltage, in volt  
 $A$  is the electrode surface area in  $\text{cm}^2$ .

The recombination constant  $k'$  is given [2] by the Smoluchovsky equation

$$k' = 4\pi r_c (D_+ + D_-) = 4\pi r_c D, \quad /1.5/$$

where  $r_c$  is the effective collision radius of the oppositely charged ions, while  $D_+$  and  $D_-$  stand for the diffusion coefficients of the positive and negative ions, respectively.  $r_c$  in Eq. /1.5/ is the critical distance at which the energy  $\frac{e^2}{r_c \epsilon}$  of the coulombic interaction between oppositely charged ions is balanced by their thermal energy  $kT$ ; that is

$$r_c = \frac{e^2}{\epsilon kT}, \quad /1.6/$$

where  $\epsilon$  is the static or a complex dielectric constant, depending on the relative rate of the relaxation and recombination processes. The diffusion coefficient can be evaluated from Einstein's relation

$$D = \frac{\mu kT}{e} \quad /1.7/$$

From this  $k'/\mu = \frac{4\pi e}{\epsilon} = 1.81 \times 10^{-6}/\epsilon$ , which on substitution into Eq. /1.3/ gives a simple expression for the calculation of the free ion yield in irradiated systems:

$$G_{fi} = \frac{1.8 \times 10^{-4} \sigma^2}{\dot{D} \mu \epsilon} \quad /1.8a/$$

The appropriate units for  $\sigma$  in Eq. /1.8a/ are  $\text{ion cm}^{-1}\text{volt}^{-1}\text{sec}^{-1}$ . If the conductivity is expressed in  $\text{ohm}^{-1}\text{cm}^{-1}$  units we get

$$G_{fi} = \frac{7.07 \times 10^{-33} \sigma^2}{\dot{D} \mu \epsilon} \quad /1.8b/$$

1.2. The effect of viscosity and pressure on  $G_{fi}$

The structure-dependent parameters  $\mu$  and  $\epsilon$  in Eq. /1.8/ vary with the temperature and pressure of the system. The ion mobility is sensitive to changes in the viscosity of the irradiated substance. In the case of dielectric liquids this dependence can be described for negative ions by reformulation of the Stokes-Walden law as  $\mu_- = f \eta^{-1}$ , while for positive ions Adamczewski's empirical formula [3]  $\mu_+ = f \eta^{-3/2}$  can be used. On substituting these expressions for  $\mu$  into /1.8/, taking the rest of the parameters to be constant, we get [3]

$$\begin{aligned} i_- &\propto k \eta^{-0.5} & \text{and} \\ i_+ &\propto k \eta^{-0.75} \end{aligned} \quad /1.9/$$

for the current of negative and positive ions, respectively. Since the mobilities of positive and negative charge carriers in dielectric liquids are usually of the same order of magnitude /in most cases  $\mu_- \approx 1.5 \mu_+$ /, one can write [4]

$$(\mu_+ + \mu_-)^{0.5} \propto \eta^{-0.6} \quad /1.10/$$

Hence at room temperature  $G_{fi}$  is expected to be nearly the same for any nonpolar liquid. However, in the case of polar liquids with different dielectric constants /alcohols, ethers, substituted aromatics, etc./ the values of  $G_{fi}$  can be markedly different.

All the variables in Eq. /1.8/ are pressure dependent. The free ion yield at pressure  $p$  is expressed [5] relative to the yield per bar, as

$$\frac{G_{fi}^p}{G_{fi}^1} = \frac{\dot{D}_1 \mu_1 \epsilon_1 \sigma_p^2}{\dot{D}_p \mu_p \epsilon_p \sigma_p^2} \quad /1.11/$$

Since  $\dot{D}$  is directly proportional to the density  $\rho$  of the liquid and providing the Stokes-Walden relation holds, /1.11/ can be written

$$\frac{G_{fi}^p}{G_{fi}^1} = \frac{\rho_1 \eta_p \epsilon_1 \sigma_p^2}{\rho_p \eta_1 \epsilon_p \sigma_1^2} \quad /1.12/$$

For nonpolar liquids  $\mu$  in Eq. /1.8/ can be expressed as

$$\mu = \mu_0 \exp \left( - \frac{W}{kT} \right), \quad /1.13/$$

where  $W$  is the activation energy for the drift of charge carriers.  $\sigma$  can thus be introduced into Eq. /1.13/ in its usual form

$$\sigma = \sigma_0 \exp\left(-\frac{W}{2kT}\right), \quad /1.14/$$

with  $\sigma_0$  including both  $\dot{D}$  and  $\epsilon$ , which may vary slightly with temperature and might thus be responsible for the different slopes of the curves  $\ln \sigma$  vs  $T^{-1}$  measured for different nonpolar materials. It has been observed in a large number of experiments [3,6,7] that

$$W_+ = \frac{3}{2} W_\eta, \quad /1.15/$$

which means that the activation energy  $W_+$  for the displacement of positive charge carriers is higher than the activation energy  $W_\eta$  needed for neutral molecules.

## 2. EVALUATION OF THE FREE ION YIELD $G_{fi}$

### 2.1. Range-energy relation for electrons

Up to a critical value of the applied field the current generated by irradiation is proportional to the product of the mobility and the number of electrons escaping recombination. The electron escape probability obviously increases with the distance  $r$  between the positive ion and the electron. For an isolated pair of singly charged ions the escape probability in the absence of an applied field is given in the Onsager theory [8] as

$$\phi(r) = \exp\left(-\frac{r_c}{r}\right), \quad /2.1/$$

where  $r_c$  is the term defined by Eq. /1.6/. The thermalization distance,  $r_c$ , of an electron depends on its initial kinetic energy and on the nature of the energy loss leading to thermalization. If the distribution function of electrons thermalized at various distances is known, the free ion yield can be evaluated, since  $G_{fi} \propto r_c$ .

The distribution function of electrons differentiated with respect to  $r$  cannot be directly measured. Calculations were made by Freeman [9] and later by Hummel and Allen [10,11], who extrapolated the experimentally determined curves of initial electron energy vs number of electrons generated at a given energy to thermal energies and evaluated the distribution of  $r$  from the plot of electron range vs energy measured for the system. Lea's [13] semi-log plot of the delta-ray energy dis-

tribution for 384 keV electrons was extrapolated from 100 eV to 0 eV in [9]. From the range vs energy curve for electrons in water the number and energy distribution of electrons per incident electron was calculated in [11] using the Bethe formulae [20] and the calculation method of Burch [21]

$$dN = \frac{n_e d\sigma}{-dT/dx} = \frac{dW_B}{2W^2 \ln(2T/I)}$$

$$-dT/dx = (2\pi n_e e^4 / T) \ln(2T/I)$$

$$d\sigma = (\pi e^4 / T) (dW/W_B^2) \quad /2.2/$$

where  $dN$  is the number of energy loss events lying between  $W_B$  and  $W_B + dW_B$  per unit total energy lost by the primary.  $I$  is the mean stopping potential of the molecules in the medium,  $n_e$  the number of electrons per unit volume,  $d\sigma$  the cross-section for electron-electron collision leading to energy losses between  $W_B$  and  $W_B + dW_B$ .  $T$  is the kinetic energy of the primary electron and  $W_B$  the energy loss.

This distribution function can be used to evaluate  $G_{fi}$  by numerical solution of the equation

$$G_{fi} = \frac{\int N(r) \phi(r) dr}{\int N(r) dr} \cdot G_{tot} \quad /2.3/$$

where  $N(r)$  is the relative number of the electrons thermalized at distance  $r$  from their parent ions. In liquids studied so far /hydrocarbons, alcohols, ethers/ the values of  $G_{tot}$  obtained from conductivity measurements were found to vary from 3 to 4 ion/100 eV.

A slightly different approximation to the free ion yield was proposed by Mozunder and Magee [12]. They studied energy partition in glancing and knock-on encounters and differentiated three types of tracks: spurs, blobs and short tracks [14,15]. Spurs are generated by electrons with energies from 6 to 100 eV, blobs by electrons of 100 to 500 eV, and short tracks by those with energies from 550eV to 5keV.  $G_{fi}$  was calculated for each of the three entities and tabulated [14] according to primary electron energy. A general expression for  $G_{fi}$  was formulated as

$$G_{fi} = \sum G_i \rho_i(T), \quad /2.4/$$

where  $G_i$  is the yield from a particular entity of given size, the index  $i$  covers spurs, blobs and short tracks of all sizes /as specified in Table [15], and  $\rho_i(T)$  is the probability that a separate charge carrier pair will result from a given entity at temperature  $T$ .

In the calculation of  $\rho_1(T)$ , it is assumed that electronic stopping dominates the energy degradation process of an electron down to the first electronic excitation energy of the solvent molecules, and that below this energy [shown to be of the order of 6 eV [16]] the electron is incapable of causing electronic transitions but loses its excess energy to the excitation of molecular vibration. As this vibrational mechanism of energy transfer is effective only down to about 0.5 eV, in the lower, so-called subvibrational state the electron energy is transferred by elastic collisions and/or by exciting intermolecular or hydrogen bond vibrations in hydrogen-bonded systems. Fig. 1 reproduces

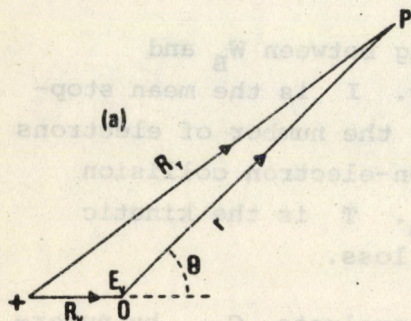


Fig. 1 a/

Thermalization in a coulombic field. Geometrical relation between the thermalization length  $R_T$ , the total random walk  $r$ , and the subvibrational distance  $R_V$ .

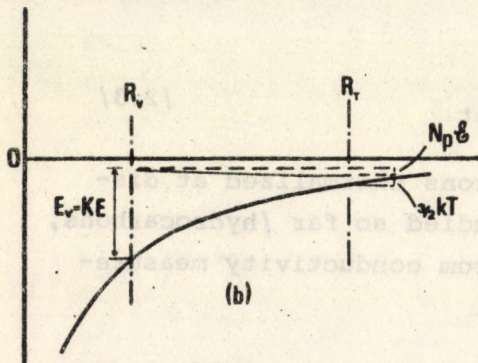


Fig. 1 b/

Energy relationship for thermalization in a coulombic field.  $E_V$  is the subvibrational kinetic energy. The energy at thermalization is  $3/2 kT$ , whereas the total loss factor is  $np\epsilon$  [16].

from [16] the energy and geometrical relationships for electron thermalization in the coulombic field of the parent ion in a nonpolar system. The electron travels a distance  $R_V$  from the positive ion before reaching its subvibrational state. If the electron is thermalized at a point P determined by the random path of length  $r$  and the angle  $\theta$  relative to the direction of the path  $R_V$ , then the thermalization length  $R_T$  is given by

$$R_T^2 = R_V^2 + r^2 + 2R_V r \cos\theta \quad /2.5/$$

If the thermalization from  $R_V$  to  $R_T$  occurs after  $n$  scattering free paths have been covered by the electron, and  $p$  is the probability of exciting an intermolecular vibrational quantum with loss  $\epsilon$  per unit scattering free path, we can write

$$E_V - \frac{e^2}{R_V} = \frac{3}{2}kT - \frac{e^2}{R_T} + np\epsilon \quad /2.6/$$

If  $L$  is the mean free path for elastic scattering, then in terms of the random walk model, for not too small  $n$ , the probability that after  $n$  steps the electron will be at a distance lying between  $r$  and  $r + dr$  from 0 /see Fig. 1a/ is defined as  $W(r,n)dr$ , where

$$W(r,n) = \left( \frac{2\pi nL^2}{3} \right)^{-3/2} \exp \left( -\frac{3r^2}{2nL^2} \right) \quad /2.7/$$

The net probability  $\rho_i(T)$  that a free ion pair will result from a given entity is a function of both the thermalization probability  $W(r,n)$  and the Onsager escape probability Eq. /2.1/:

$$\rho_i(T) = \int dr W(r,n) \phi(r,T) \quad /2.8/$$

With a given set of numerical values of the physical parameters  $E_V$ ,  $R_V$ ,  $p$ ,  $\epsilon$ ,  $L$  and  $T$ , it is possible to calculate the distribution of the thermalization lengths, the mean distance for thermalization and the mean square deviation of the latter. Calculations with the values of the parameters for hexane show that there is a gaussian distribution of the thermalization lengths, with a median to modulus ratio  $\sim 1/4$  which is essentially independent of temperature.

The gaussian distribution of the thermalization lengths, although supported only by the reasonable agreement of the predictions from the above equations with the available experimental data, does suggest that ejected electrons rapidly lose a large fraction of their energy by exciting electronic and vibrational transitions in the molecules along their path and are slowed down to subvibrational energies at a distance of 10-20 Å from their parent ions. The subsequent path of the electrons up to final thermalization /from  $\sim 0.4$  to 0.025 eV/ is governed by a process very similar to diffusion and is substantially longer than the process of energy loss to subvibrational energy, and the path length distribution of these electrons can be considered truly gaussian.

Assuming that the thermalization length does not depend appreciably on the initial energy of the electron and that its distribution can be described by the three-dimensional gaussian distribution function  $(4\pi r^2/\pi^{3/2}b^2)e^{-r^2/b^2}$ , Schmidt et al. [17] calculated the escape probability,  $P$ , given by the product of the gaussian distribution and the Onsager escape probability,  $\exp\left(-\frac{r}{c}\right)$ , from

$$P = \frac{4}{\pi^{1/2}} \int_0^{\infty} x^2 \exp \left[ -x^2 - \frac{r_c}{bx} \right] dx, \quad /2.9/$$

where  $x$  has been substituted for  $r/b$ . As can be seen,  $P$  varies only with the ratio  $b/r_c$ , the values of which have been calculated and tabulated [17,18]. In this expression,  $b$  is the average thermalization length, i.e. the ordinate for the median of the distribution curve, and can be evaluated from  $b/r_c$ , since  $r_c$  is given by Eq. /1.6/; it is related to the penetration length of the electrons in the liquid, which is known to be inversely proportional to the density  $\rho$ . Thus, the product  $b\rho$  for similar compounds /e.g. saturated hydrocarbons/ is expected to be constant. This prediction seems to be consistent with the experimental data obtained so far.

The product  $b\rho$  is a statistical parameter of the interaction between slowing-down electrons and the medium and seems to be independent of temperature for a given liquid.

## 2.2. The time dependence of $G_{fi}$

Electrons and negative ions can be divided into two groups according to their thermalization lengths, by classing in the first group those which cannot and in the second those which can escape geminate recombination. The lifetime of ions of the first group is determined by electrical forces to a greater extent than that of ions of the second group, which disappear by second order recombination kinetics.

The relative velocity  $v$  of a pair of oppositely charged ions during recombination can be expressed [19] as

$$v = -E\mu = -\frac{e(\mu_+ + \mu_-)}{\epsilon r^2 4\pi} = \frac{1.44 \times 10^{-7} (\mu_+ + \mu_-)}{\epsilon r^2}, \quad /2.10/$$

where  $\epsilon$  is the dielectric constant, and  $r$  is the distance /cm/ between the ions of a pair. The time  $t_{gn}$  taken by the geminate neutralization of ions separated initially by a distance  $r$  is given by the formula

$$t_{gn} = \int_r^{r_0} \frac{dr}{v} = \frac{\epsilon(r^3 - r_0^3)}{4.32 \cdot 10^{-7} (\mu_+ + \mu_-)}, \quad /2.11/$$

where  $r_0$  is the minimum distance at which the charge transfer takes place. It is probable that  $r \gg r_0$ .

The half-life of the ions which are neutralized at random by second order kinetics is given as

$$t_{1/2} = \frac{1}{k'n_0}, \quad /2.12/$$

where  $n_0$  is the initial concentration of both negative and positive free ions, and  $k' = \frac{4\pi e\mu}{\epsilon} \text{ cm}^3 \text{ sec}^{-1}$  and can be estimated [19] from

$$k' = 3.32 \cdot 10^{-11} / \epsilon \eta \quad \text{cm}^3 / \text{sec} \quad /2.13/$$

where  $\eta$  is the viscosity, in poise, of the liquid.

The concentration of the migrating charge carriers, i.e. the current which can be observed at time  $t$  after a short irradiation pulse or after a long continuous irradiation period, is composed of the contributions from ions not yet geminately recombined and from the "free" ions diffusing in the system at random. Thus the radiation chemical yield can be expressed as

$$G_t^- = G_t^1 + G_t^2, \quad /2.14/$$

where the superscripts 1 and 2 denote the two types of contributions. For the evaluation of  $G_t^-$  Freeman [19] has introduced the formula

$$G_t^2 = G_0^2 \cdot F_{fi}(t), \quad /2.15/$$

where

$$F_{fi}(t) = (1 + n_0 k' t)^{-1}, \quad /2.16/$$

is the fraction of free ions still surviving at time  $t$ . Log  $i$  vs log  $t$  and the time curves for the ratio  $G_t^- / G_0^-$  ( $G_0^-$  is the negative charge carrier yield at time  $t = 0$ ) are shown in Figs. 2 and 3 for different nonpolar and polar systems. It can be seen that in nonpolar cyclohexane geminate recombination takes place in  $10^{-11}$  secs, while in the polar water, ethanol and acetone the process takes  $10^{-10}$  secs.

It has been questioned which value of  $\epsilon$  should be used for the evaluation of  $G_t^-$ . The dielectric constant of a system is time dependent in so far as a given time is required by the molecular dipoles to turn and

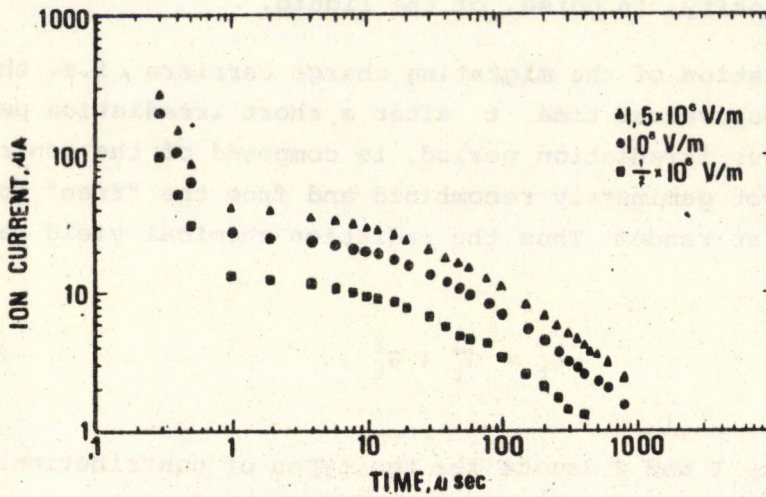
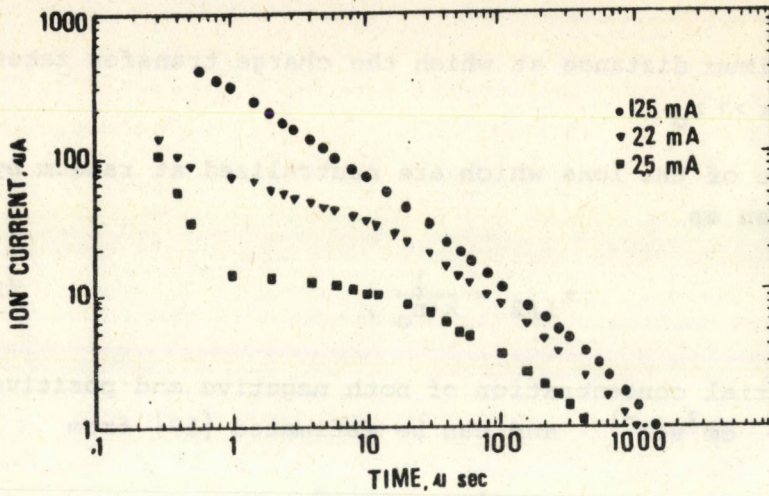


Fig. 2

Current vs time in hexane for various collecting fields and a delivered charge of  $2.5 \times 10^{-10}$  coulomb [37]

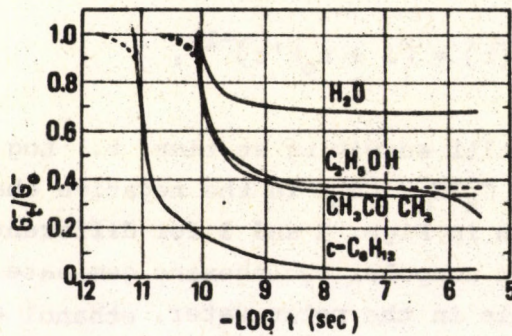


Fig. 3

Calculated spectra of lifetimes of solvated electrons after applying an instantaneous pulse/100 rads/ of high-energy electrons or X-rays to pure water, ethanol, acetone and liquid cyclohexane at 20°C. The dashed curves on the left side of the figure were drawn arbitrarily [19]

be aligned in the direction of the electric field. If the time of the interaction between the electric field of an ion and a dipole is sufficiently long for this alignment to be completed, a static dielectric constant can be assumed to exist. However, for a dielectric relaxation time,  $\tau$ , close to or longer than the interaction time constant /depending primarily on the lifetime  $t_{gn}$  and on the velocity of the ions/ only partial or no reorientation at all can take place, and in this case a time-dependent dielectric constant has to be used [19], as given by

$$\epsilon(t) = \epsilon_0 + \frac{\epsilon_\infty - \epsilon_0}{1 + (\tau/t)^2}, \quad /2.17/$$

where  $\epsilon_0$  and  $\epsilon_\infty$  are the values of the dielectric constant at  $t = 0$  and  $t = \infty$ , respectively. /These must not be confused with the symbols used for static and infrared dielectric constants./ The value of the dielectric constant averaged over the time from  $t = 0$  to  $t = t_{gn}$  can be obtained as

$$\bar{\epsilon} = \int_0^{t_{gn}} \epsilon(t) dt / \int_0^{t_{gn}} dt = \epsilon_\infty - (\epsilon_\infty - \epsilon_0) \left( \frac{\tau}{t_{gn}} \right) \tan^{-1} \left( \frac{t_{gn}}{\tau} \right) \quad /2.18/$$

The values of  $\tau$  involved in the above equations for  $\epsilon(t)$  are probably smaller than those measured by the usual microwave techniques, since the sudden production of a charge carrier in an irradiated system very probably intensifies the thermal motion of the neighbouring molecules and facilitates the alignment of the dipoles. The average torque  $U$  exerted by a singly charged ion on a molecule with dipole moment  $\omega$  lying at a distance  $r$  in a medium with dielectric constant  $\epsilon$  can be roughly approximated as

$$U = \int_0^{\pi/2} \frac{e\omega}{\epsilon r^2} \sin\theta \, d\theta / \int_0^{\pi/2} d\theta = 0.64 \frac{e\omega}{\epsilon r^2} \quad /2.19/$$

Comparison of the predicted time dependence of the ratio  $G(e^-_{solv})_t : G(e^-_{solv})_0$  with the experimental values for ethanol shows a decrease in the dielectric relaxation time in the vicinity of the ions by a factor from 5 to 10. For details see [19, 20, 21].

### 3. METHODOLOGY

#### 3.1. Measurement of steady-state current

The resistivity of the compounds studied by conductivity measurements under irradiation varies from  $10^8$ - $10^{20}$  ohm.cm. The radiation-generated current,  $i$ , in Eq. /1.8/ is given by the difference between the current measured during irradiation and the dark current. Since this increase in current is easier to measure if the dark current is low, dielectric liquids with  $\sigma = 10^{-16}$  to  $10^{-20}$  ohm<sup>-1</sup>cm<sup>-1</sup> have been preferred in these studies.

The accurate measurement of such high d.c. resistances is quite a difficult task and not only a highly sensitive electrometer but also some special experimental precautions are required. Most of the d.c. measurements were performed by using two electrodes only. In this case the current produced by the voltage  $V$  applied to the electrodes is measured both before and during irradiation. The d.c. conductivity  $\sigma$  is evaluated from the formula

$$\sigma = \frac{iL}{AV} ,$$

where  $L$  is the electrode spacing /cm/ and  $A$  is the area /cm<sup>2</sup>/ of the electrode surfaces.

Galvanometers with sensitivities from  $10^{-10}$  to  $10^{-11}$  amp/unit scale are suitable for the measurement of resistivities up to  $10^{16}$  ohm cm, but they are now being increasingly replaced by highly refined d.c. electrometers and vacuum tube voltmeters incorporating solid-state electronics. The input resistance of these latter meters can be as high as  $10^{16}$  ohms, with an input grid current of less than  $5 \times 10^{-14}$  A, a typical input capacitance of 30 pF and a zero drift of about 200 microvolts/day. Of course, the use of such high sensitivity electrometers requires much attention to response times and to protection from stray fields and noise.

The response times of both the electro- and voltmeters are given by the product of the input resistance  $R$  and the input capacitance  $C$ . Taking, for example, an electrometer measuring a decrease in voltage of 1 V across a resistor of  $10^{13}$  ohm /see Fig. 4/, the response time  $RC = 10^{13}$  ohm  $\times$   $3 \cdot 10^{-11}$  Farad = 300 sec. The rise time of the output voltage from the electrometer is determined [22] by the ratio

$$\frac{E_t}{E_o} = \left[ 1 - \exp \left( \frac{t}{RC} \right) \right] \quad /3.2/$$

where  $E_t$  and  $E_o$  are the potentials of the electrometer at time  $t$  after switching-on and of the voltage supply, respectively.

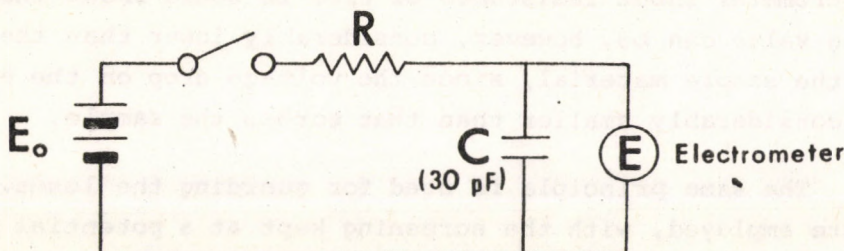


Fig. 4

Schematic arrangement of the circuit for measuring current in dielectrics

An input capacitance of 30 pF is typical for vibrating reed electrometers and is generated by the input leads, the wiring and the effective input capacitance of the tube grid. Since it is customary to take readings after a time equal to four or five times  $RC$ , one has to wait for 20 to 25 minutes to obtain accurate values, This waiting time is practicable only if the electric parameters of the sample do not change faster than the time constant of the apparatus.

Since in many cases /e.g. pulse conductivity measurement, current measurement in very viscous liquids, or during the heating of irradiated glasses/ the change in sample resistivity takes less time than the time constant of the conventional measuring circuits, the readings must be carefully interpreted, or the effect has to be suppressed by reducing  $C$  or  $R$ , or both.  $C$  can be minimized by keeping the input leads as short as possible and by placing the grounded shielding as far as possible from the live conductor connecting the sample to the electrometer input.

The reduction of  $R$  requires a corresponding increase in the voltage sensitivity of the electrometer or in the value of the applied voltage. An increase in sensitivity usually leads to a higher noise level and zero drift. Increases in applied voltage are limited by the change of the kinetics of the process during irradiation in the higher applied fields, or, in some cases, by breakdown of the material studied.

Readings can also be falsified by electrode effects and surface currents. These can be minimized by the use of a grounded guard ring mount-

ed around the electrode connected to the electrometer terminal. This guard ring collects all surface currents and leads them to the ground. The current flowing between the guard ring and the measuring electrode is too small to affect the value of the measured current, its value being determined by the voltage drop /usually not more than 1 V/ across the electrometer and the resistance of the material between the guard ring and the electrode. This resistance must be several orders of magnitude higher than the electrometer input resistance or else it would shunt the measuring device. Its value can be, however, considerably lower than the bulk resistance of the sample material, since the voltage drop on the electrometer is also considerably smaller than that across the sample.

The same principle is used for guarding the leads. Screened cables are employed, with the screening kept at a potential close to that at which the current is measured, in order to minimize current leakage.

Electrometers are extremely sensitive to small transient electric fields produced by fluctuations due to switching or to the operation of motors or a.c. devices. Usually the electrometers do not respond to a.c. signals of less than 1 cps, but even so shielding seems to be a practical necessity in all cases. The shielding is usually a grounded, vacuum-tight metal box housing the measuring circuit. This shields the device against electric field effects but does not provide any protection against the magnetic fields that are frequently generated in pulse experiments when large capacitors are discharged.

Unfortunately, the use of long cables, which increase the input capacitance of the electrometer and which are sensitive to spurious fields, cannot be always avoided without exposing the instruments and personnel to radiation hazards. In this case, care must be taken to prevent any movement of the cable, since friction and sliding of the insulation may induce spurious potentials on the central conductor and increase the capacitance of the measuring setup. These cable effects can be minimized by the use of special "low noise" cables and the differential cancellation method used by Tewari et al. [49].

### 3.2. Mobility measurement

Electrical conductivity depends on both the concentration and the mobility of the charge carriers. The mobility  $\mu$  is defined as the mean velocity of the charge carriers in the field direction per unit applied field; i.e.  $\mu = \frac{v}{E}$ . The mean velocity of the charge carriers is calculated by dividing the distance covered by the time the charge carriers keep mov-

ing plus the time they are in trapped state. Thus mobility is a function of the concentration and depth of the traps, too.

The mobility is usually evaluated by measuring the time taken by the charge carriers to travel a given distance in the system under investigation. In the classic experiments of LeBlanc [23], electrons were photoejected from a highly polished Al cathode by an intense pulse of UV light, and the time taken by the photoelectrons to reach the anode was measured. The duration of the light flash had to be short compared to the transit time of the electrons.

A thin layer of charge carriers parallel to the electrodes can be produced at any point between them by a narrow X-ray or electron pulse directed at the desired point. Such thin pulses can be obtained from a pulsed X-ray machine or an electron accelerator. The accelerated beam of electrons is used either to strike the sample directly across a slit, or to release from a metal target an X-ray pulse which is then directed onto the sample. This pulse technique was used to obtain the most recent experimental data.

A useful method for measuring the mobility of natural charge carriers which are responsible for the dark current has been described by Lewa [24] and improved by Kleinheins [25]. The technique /see Fig. 5/ is to apply two forces to the charge carriers: an electric field between the elec-

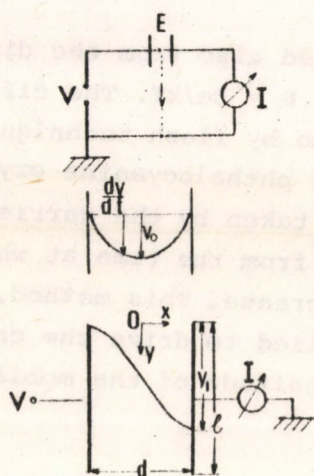


Fig. 5

Schematic circuit diagram and measuring arrangement showing the path of an injected charge carrier starting from the top of the left electrode. /E= measuring electrode./

trodes drives the carriers at a velocity  $v_x = \mu E$  in the direction perpendicular to the electrode surface, while the liquid flowing through the measuring cell drives them at a velocity  $\bar{v}_y$  parallel to the surfaces. The value of the measured current is at a maximum when the liquid between the electrodes is at rest and decreases proportionally to the increase in the flow rate of the liquid. For each type of carrier there exists a critical velocity of the liquid at which all the charges are removed before reaching the electrode surface and the current thus becomes virtually zero. The time  $t_0$  needed by the electrons to cover the distance  $d$  between the electrodes can be es-

timated from the critical velocity  $v_c$ , as

$$t_l = \frac{l}{\bar{v}_c} ,$$

where  $l$  is the length of the measuring electrode, and the mobility of the carriers is given by the formula

$$\mu = \frac{\bar{v}_x}{E} = \frac{d}{t_l E} = \frac{d\bar{v}_c}{lE} = \frac{d^2\bar{v}_c}{lV} . \quad /3.3/$$

The true picture is, however, more complicated because of the parabolic velocity distribution between the electrodes. The detailed analysis is given in the original papers [24,25].

It follows from the above that if a liquid moves in the direction of the applied field this may cause an error in the current measurement. It has been shown that electric currents as low as  $10^{-11}$  A can cause the bulk liquid to move at a velocity similar to that of the charge carriers. It was pointed out, therefore, by Essex and Secker [26], that the induced liquid motion has to be taken into consideration when estimating the mobility from the measured transit time. These authors used a special measuring cell and circuit which permitted the displacement of the carriers in the direction of the electrode surface /apparent mobility/ to be distinguished from that corrected for bulk liquid displacement /true mobility/.

The carrier mobility can be estimated also from the diffusion constant by making use of Einstein's formula  $\mu = De/kT$ . The diffusion method was used by Kearns and Calvin [27], who by flash technique generated charge carriers on the rear surface of a phthalocyanine crystal having electrodes on its opposite surface. The time taken by the carriers to diffuse through the crystal could be determined from the time at which the current between the electrodes started to increase. This method, which differs from the others in that no field is applied to drive the carriers, is suitable only for estimating the order of magnitude of the mobility, and its use is restricted to solids.

### 3.3. Charge carrier lifetime

Charge carrier recombination is a second order process, and thus after irradiation has been stopped the decrease in concentration caused by recombination can be expressed /see Eq. 1.2/ as

$$-\frac{dn}{dt} = k'n^2 , \quad /3.4/$$

where  $n$  is the concentration of a given type of carrier. The solution to the differential equation gives

$$\frac{1}{n} = \frac{1}{n_0} + k't \quad /3.5/$$

Since

$$\sigma = \mu en = \frac{iL}{VA} \quad , \quad /3.6/$$

thus

$$\frac{1}{i} = \frac{1}{i_0} + \frac{k'}{\mu} \frac{Lt}{AV} \quad /3.7/$$

The experimental value of  $k'/\mu$  can be evaluated from the plot of  $i$  vs time, since the combination of Eqs. 2.12 and 6.6 gives

$$t_{1/2}\sigma_0 = \frac{\mu e}{k'} = \frac{\epsilon}{4\pi} \quad /3.8/$$

which after the introduction of a dimensional factor takes the form

$$\frac{k'}{\mu} = \frac{1.6 \cdot 10^{-19}}{t_{1/2}\sigma_0} \quad /3.9/$$

If  $\mu$  is in  $\text{cm}^2 \text{volt}^{-1} \text{sec}^{-1}$ ;  $t_{1/2}$ , the half-life of the free ions, is in sec;  $\sigma_0$ , the conductivity of the system at  $t=0$ , is in  $\text{ohm}^{-1} \text{cm}^{-1}$ ; then  $k'$  is obtained in  $\text{cm}^3 \text{sec}^{-1}$  units. The experimental values so far obtained seem to fit the relationship  $k'/\mu = 4\pi e/\epsilon$ .

#### 4. FACTORS OTHER THAN RADIATION AFFECTING THE CONDUCTIVITY

##### 4.1. The role of electrodes

It is well known from electrochemistry that electrode properties such as material, structure, impurities, surface state, oxide layer, etc. play an important role in the kinetics of electrode processes. The same is true for semiconductors and it is considered a great art to find suitable electric contacts. The theories of electrode-electrolyte, electrode-semiconductor or n-p type junction interactions have not been considered so far in the calculation of currents generated in dielectric organic liquids. The importance of the electrodes in conductivity measurements can be best understood if one treats the system as a junction between metal and semiconductor material. This is justified because the release of ions and

the formation of holes and traps in the irradiated system transform the dielectric organic materials into semiconductors. Electron transfer at electrodes occurs either from the metal to the sample /cathode/ or from the sample to the metal /anode/. The separate work functions of the electrode and semiconductor determine the processes occurring when the two different materials are brought into contact. The work function is the energy needed to remove the electron infinitely from the Fermi level /chemical potential/ and is specific for each system. Since in semiconductors there are no electrons at the Fermi level lying between the valence and conduction bands, electrons have to be removed from both valence and conduction bands in order to prevent any change in temperature.

If two materials are brought into contact, the electrons will flow from the material with lower to that with higher work function; opposing this current is the potential caused by the excess electrons and positive holes /forming a double layer near the interface/ which builds up until equilibrium is reached. The situation is illustrated schematically in Fig. 6.

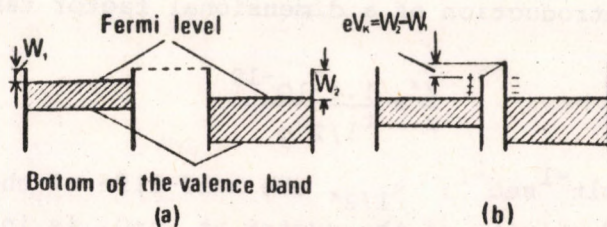


Fig. 6

Scheme of contact potential formation

Let the work function of the metal be higher than that of the n-type semiconductor /Fig. 7/. Upon contact the electrons will flow from

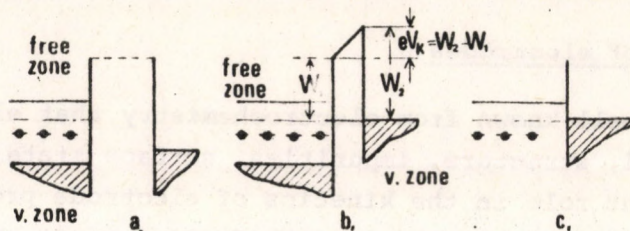


Fig. 7

Metal n-type semiconductor barrier layer  
 a/ energy levels before equilibrium  
 b/ the potential change across the boundary after equilibrium  
 c/ schematic representation of the barrier

the semiconductor to the metal. This flow of electrons continues until it is levelled out by the field of the double layer formed at the interface. After equilibrium is reached the metal is negatively charged at the contact, while the semiconductor surface contains, to a certain depth, positively charged ionized donors /Fig. 8/. The electric field formed by the two types of layers is called a barrier [28,29].

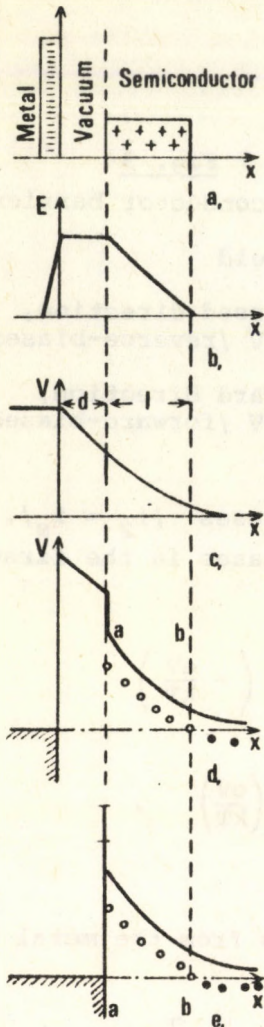


Fig. 8

Metal n-type semiconductor barrier layer with regard to space-charge

- a/ charge distribution
- b/ field intensity
- c/ potential change if the potential drop at metal-semiconductor junction is not considered
- d/ potential change if the potential drop at metal-semiconductor junction is considered
- e/ schematic representation of the junction

In the equilibrium state the chemical potentials /Fermi levels/ of the metal and the semiconductor are the same. The electron current from the metal to the semiconductor remains unchanged during the formation of the barrier,

while that from the semiconductor to the metal decreases because of the ever higher energies needed by the electrons to surmount the potential gradient  $V_k$  between the two materials and the energy determined by the work function of the semiconductor [30]. The two currents are in equilibrium if

$$i_{s1} = A \exp - \left( \frac{eV_k + W_1}{kT} \right) = i_{s2} \quad /4.1/$$

so the net current  $i = i_{s1} - i_{s2} = 0$ .

The applied voltage can either increase /Fig. 9a/ or decrease /Fig. 9b/ the energy barrier. As is apparent from Fig. 9, the current from the metal

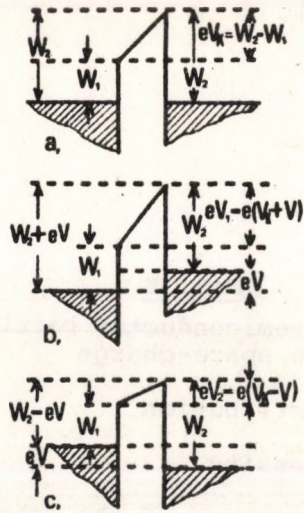


Fig. 9

Metal n-type semiconductor barrier layer

- a/ no applied field
- b/ field in reversed direction,  
 $eV_1 = eV_k + eV$  /reverse-biased/
- c/ field in forward direction,  
 $eV_2 = eV_k - eV$  /forward-biased/

to the semiconductor has the same value in both cases  $|i_2 = i_s|$ . But the current from the semiconductor to the metal decreases in the first and increases in the second case, thus

$$I_1 = A \exp \left( - \frac{W_1 + eV_k + V}{kT} \right) = I_s \exp \left( - \frac{eV}{kT} \right) \quad /4.2/$$

and

$$I_2 = A \exp \left[ - \frac{W_1 + e(V_k - V)}{kT} \right] = I_s \exp \left( \frac{eV}{kT} \right) \quad , \quad /4.3/$$

respectively.

The resulting net current in the first case flows from the metal to the semiconductor

$$I = I_1 - I_2 = I_s \left[ 1 - \exp \left( - \frac{eV}{kT} \right) \right]; \quad /4.4/$$

and in the second from the semiconductor to the metal

$$I = I_2 - I_1 = I_s \left[ \exp \left( \frac{eV}{kT} \right) - 1 \right] \quad /4.5/$$

Thus the junction acts as a rectifier, since the current increases exponentially with the forward-biased applied voltage and goes asymptotically to  $I_s$  in the case of reverse bias.

If the work function of the metal is lower than that of the n-type semiconductor, no barrier forms on their contact. This type of contact is referred to as ohmic, since the current is not rectified and Ohm's law holds over a wide range of the applied voltage. For a p-type semiconductor to have an ohmic contact, the work function of the metal must be higher than that of the semiconductor.

The effect of the contact between the electrode and the dielectric liquid has not yet been considered in the estimation of the currents measured in the liquid, since the two electrodes are usually made of the same metal, which excludes the observation of any rectifying action. The differences between the currents measured on the same material by workers using different pairs of electrodes have usually been attributed to variations in the impurities in the samples and the electrode-liquid contact effect has not been taken into account.

A theoretical approach to the problem is difficult because the work functions for electron release into a dielectric system are unknown. The formation on the semiconductor of a surface layer or a thin oxide layer may also give rise to contributions which are practically impossible to evaluate. It seems nevertheless reasonable to assume that the energy required to release an electron into a dielectric is appreciably less than that needed for the release into vacuum, particularly if the dielectric constant of the system is high. In fact, for higher values of the dielectric constant, correspondingly higher values of conductivity have usually been observed. To a first approximation, the work function for release of an electron from the metal into vacuum  $W_m$  less the electron affinity  $\kappa$  of the liquid can be used as a work function for release into the liquid [31,32].

#### 4.2. Potential distribution in the conductivity cell

In an overwhelming majority of treatments the potential distribution between the electrodes is assumed to be uniform. This, however, is far from being true [33], since the actual value of the electric field may substantially deviate from the mean /Fig. 10/ and thus result in an apparently unusual electron behaviour.

The deviation from an even potential distribution is due to the accumulation of charge carriers /space charge/ in the cell and on the electrode surfaces. This accumulation is observed whenever the carriers cannot be neutralized for some reason, e.g. they are already surrounded by neutral molecules upon their arrival at the electrode. Space charge may result in the increase of the local electric field, which may lead

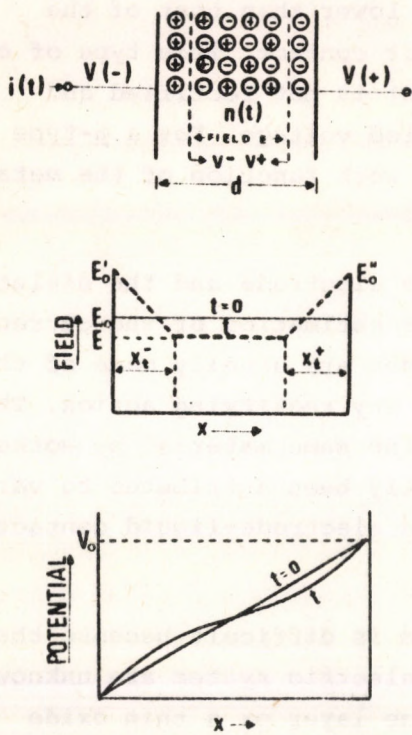


Fig. 10

Approximate potential distribution in the cell at  $t=0$  and time  $t$  latter

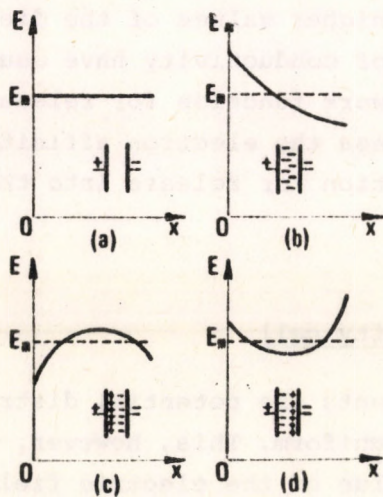


Fig.- 11

The possible cases of space charge distributions

in turn to secondary electron emission or to the breakdown of the solvate shell by electrostatic forces. The magnitude of the local field depends on the strenght bond of the bond between the shell and the central ion; waker bonds are disrupted and the ions neutralized at lower fields.

The carriers accumulated not only at the electrode of opposite sign but for a short time also at the electrode at which they are formed. Thus, we can distinguish between homo-charges and heterocharges. Since the former are quickly driven to the opposite electrode, their contribution to the measured current is always transient. The possible space charge distributions are illustrated in Fig. [11].

During space charge formation the current exhibits a continuous variation, a well-known phenomenon whenever voltage is applied to a dielectric. The initial current decreases by many orders of magnitude before the eventual minute steady-state current is established. Because of these transient conditions, it is important to distinguish the electric current,  $i$ , flowing through the measuring /external/ circuit from the conduction current,  $j$ , in the dielectric, to which the former is related by

$$i = j + \frac{\epsilon}{4\pi} \frac{\partial E}{\partial t} ,$$

where  $j$  and  $E$  depend on both time and electrode spacing, and  $i$  is a function of time only. The quantity of radiation chemical interest is  $j = eE n(\mu_+ + \mu_-)$ ; its differentiation from  $i$  is sometimes, e.g. during a pulse, quite difficult.

The space charge effects on the kinetics of electric currents seem to be unduly neglected. Experimental observations dating as far back as the thirties suggested the potential usefulness of these effects for the study of ionic processes. These early data revealed the complicated mechanism of space charge formation and indicated the importance of impurities in this process /and, consequently, in the conduction mechanism too/. Space charge formation was first observed by Dantscher [34], in very pure chlorobenzene to which an electric field was applied. The negative carriers disappeared in a few seconds from the initial hetero-space charge, while the disappearance of the positive carriers took a longer time so that a uniform field distribution was established only after 30 minutes. During repeated use of a sample some impurities formed, and thus only positive space charge formation could be observed. The same compound was investigated later by Croitoru [35]. He found that the electric field was initially uniform /20  $\mu$ sec/ and that formation of a homo-space charge at both electrodes was observed only later /140-650  $\mu$ sec/. Thereafter the contribution from negative carriers became predominant throughout the entire volume and resulted in a considerable hetero-space charge at the anode. Under steady-state conditions the space charge was found to be negative in the entire volume and the electric current was limited by the rate at which these carriers were neutralized at the anode.

A special case of space charge formation occurs in pulse radiolysis. On exposure of a conductivity cell, with a field  $E_0$  between the electrodes, to a short, single burst of ionizing radiation, the ions produced with charge density  $\rho$  and mobility  $\mu$  start to recombine and during this process they are driven by a force  $eE$  towards the corresponding electrodes. The ions move at a velocity  $\mu E$  in opposite directions; thus the boundaries of the neutral central recombination zone /in which the charge densities of the positive and negative ions are equal/ move toward each other at a speed  $[\mu_+ + \mu_-] E$ , leaving a hetero-space charge layer at both electrodes [36]. Schematic graphs of the ion, field and voltage distributions at  $t = 0$  and a short time later are shown in Fig. 10. The internal field, uniform before the pulse, is changed by the formation of space charge, which shields the bulk recombining zone, and thus  $E$  decreases in the bulk system but increases at the electrodes. The space charge density is also changed by the continuous recombination, which decreases the surface charge density and the charge density of the consecutive heterocharge layers by  $\mu \rho \int_0^t E dt$ , where  $\rho$  decreases with time. Assuming constant net charge density in the homocharge layers, Gregg and Bakale [37] have shown by using a general set of equations for ionization conduction that  $\rho$  is independent of the applied field and that it decays with time at any point at either end of the neutral zone as

$$\frac{d\rho}{dt} = -(\mu/\epsilon)\rho^2, \quad /4.6/$$

while within the neutral zone it varies as

$$\frac{d\rho}{dt} \cong -\frac{(\mu_+ + \mu_-)}{\epsilon} \rho^2 \quad /4.7/$$

Since  $(\mu_+ + \mu_-) > \mu^+$  or  $\mu^-$ , the charge density decreases somewhat more rapidly in the middle than in the boundary regions. This leads to a non-linear dependence of the field on distance in the heterocharge layers. In the above expressions the possible electrode effect on the charge transfer from the layers to the electrodes has not been taken into account, so the variation of  $\rho$  in the different layers is, in fact, more complicated.

To estimate the space charge effect [37], it is assumed that  $\mu^+ + \mu^- = \mu$ , and that  $\mu$  is independent of  $E$ , the field in the neutral zone, while the space charge density  $\rho$  does not vary with the distance from the electrode of the layers and is given at any time by /4.6/. The thickness of either of the heterocharge layers  $X_t^-$  and  $X_t^+$  is given by  $X_t \cong \mu \int_0^t E dt \cong \mu Et$ . Starting from

$$V_0 = \int_0^d E dx = Ed + X_t(E'_0 - E), \quad /4.8/$$

the calculations lead to

$$\epsilon d \frac{dE}{dt} = -2\mu^2 E \rho(t) \int_0^t E dt \left[ 1 + \frac{\int_0^t E dt}{2E\rho(t)} \frac{d\rho(t)}{dt} \right], \quad /4.9/$$

which for  $0 < X_t < d/2$  gives

$$R = \frac{E}{E_0} = \frac{1}{1 + \left[ \mu^2 \rho_0 E_0 t^2 / d(\epsilon + \mu \rho_0 t) \right]} \quad /4.10/$$

Fig. 12 shows the predictions from eq. /4.10/ for  $\mu = 3.10^{-4} \text{ cm}^2 \text{ volt}^{-1} \text{ sec}^{-1}$ ,  $\epsilon = 2.10^{-13} \text{ coulomb volt}^{-1} \text{ cm}^{-1}$ ,  $E_0 = 2.10^6 \text{ volt cm}^{-1}$  and  $d = 0.2 \text{ cm}$ . It is apparent that the decrease in the applied field in the neutral zone is negligible up to 1 msec, even for infinite charge density.

It can be easily seen that recombination ceases after a time

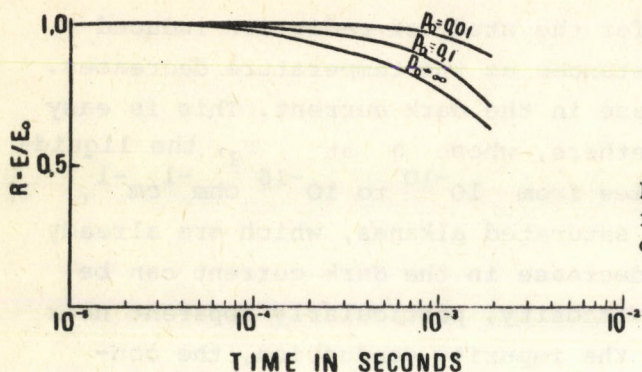


Fig. 12

Ratio of neutral zone field E to field at  $t_0 = 0$   $E_0$  as a function of time, for various charge densities

$$\tau_r = \frac{d}{(\mu_+ + \mu_-) E} \quad /4.11/$$

During this period the charge density in the neutral region is given, according to Langevin [68,69], by

$$\rho(t) = \frac{\rho_0}{1 + k' \rho_0 t/e} \quad /4.12/$$

The charge removed by recombination can be expressed as

$$\rho_r = \rho_0 \left[ 1 - \frac{1}{u} \ln(1 - u) \right], \quad /4.13/$$

where

$$u = \frac{k'}{e(\mu_+ + \mu_-)} \left( \frac{\rho_0 d}{E} \right) \quad /4.15/$$

Hence, the fraction of the total charge collected is

$$f = 1 - \frac{\rho_r 100}{GD} = \frac{1}{u} \ln(1 - u) \quad /4.16/$$

where D is the absorbed dose in eV/g units.

#### 4.3. Current peaks during warmup

The liquids generally used for the study of radiation-induced conductivity transform to glassy substances as the temperature decreases. This transformation leads to a decrease in the dark current. This is easy to see, for example, in alcohols and ethers, whose  $\sigma$  at  $T_g$ , the liquid-to-glass transition temperature, varies from  $10^{-10}$  to  $10^{-16}$  ohm<sup>-1</sup>cm<sup>-1</sup>, but more difficult to observe in the saturated alkanes, which are already dielectric at room temperature. The decrease in the dark current can be attributed partly to an increase in viscosity, particularly apparent near  $T_g$ , and partly to the freezing-in of the impurity conduction, the contribution from which decreases exponentially with decreasing temperature. In the glassy state the conduction mechanism changes and electronic conduction becomes dominant, since ionic movements are impossible, except perhaps in the case of structural changes to be discussed later.

The charge carrier behaviour in glasses, in contrast with that in liquids, is determined in the first place by increasing viscosity and the higher rate of trap formation, which result in a slower diffusion of charge carriers. As revealed by ESR and optical measurements, trapped carriers can remain in their traps for practically any time, whilst recombination in liquids takes place in  $10^{-9}$  to  $10^{-1}$  sec. The time spent in traps is a function of the trap depth. Shallow traps with a depth comparable to  $kT$  at a given temperature are characteristic of nonpolar glasses: deep traps - those from which electrons can be removed by energies of 1 eV or more - are found in polar glasses. The various trap depths within a sample inferred from decay kinetics suggest the presence of different types of traps. Although the processes are far from being understood, probably any kind of irregularity /fluctuations in density, vacancies, voids, impurity atoms, radicals, etc./ can act as a trap.

A large number of traps exist in glasses; in polar systems their concentration probably attains  $10^{20}$  cm<sup>-3</sup>. The trapping properties of the charges formed during irradiation are superimposed on those of the traps present before irradiation /preformed traps/. Since the cross-section for coulombic interaction is higher in the case of oppositely charged carriers than for particles and preformed traps, for a given temperature and trap depth there is a minimum distance at which oppositely charged carriers are able to escape recombination. Our measurements [38] have shown that in ethanol glass at 77°K the steady-state concentration of trapped electrons is  $10^{18}$  electrons per cm<sup>3</sup>, corresponding to a minimum distance  $d = 47$  Å between the positive and negative charge carriers.

In the first stage of irradiation the charge carriers, formed at a rate  $DG_1$ , are removed not only by recombination but also by trapping. Pulse radiolysis of glasses [39] permitted the observation that as a result of an intense pulse of  $10^{-8}$  sec duration the charge carriers captured in shallow traps are released and then recaptured in deeper traps. This fast redistribution of carriers takes place in microseconds and is manifested by changes in the optical spectrum from that taken during irradiation. This redistribution of trapped charges continues at a lower rate for minutes, hours or days, depending on the viscosity of the glass, and can be followed by the slow change of optical absorption. Charge redistribution, particularly in the time range studied in [39], could be detected by sensitive d.c. measurements. A change in conduction mechanism and in the value of the output current is expected to occur in irradiated glasses if all the available traps have been populated. This change, however, has not been observed so far.

More studies have been devoted to the changes of the postirradiation current during the warming process than to the steady-state currents measured during irradiation. On warming, current peaks are observed in different temperature ranges. As the sample temperature increases, current peaks are produced first by the carriers released from the shallow traps, then by those freed from the deeper traps [40]. The integration of the current peaks with respect to time during warming gives the number of charge carriers entering the measuring circuit. The experimental data /see Table 1/ show that the observed current peaks can be explained by taking them to be contribution from surface ionic processes only, since the movement of merely one per cent of a monolayer of charge carriers is sufficient to give the measured currents. Even so, the current peaks most probably reflect structural changes within the bulk of the glass and thus give valuable information about changes which cannot be detected by other methods /ESR, NMR/. Indeed, it seems from the similarity of the current vs temperature curves obtained on the same glass with the use of different electrodes that the peaks reflect bulk processes, since the surface processes are more sensitive to electrode effects.

Negative currents /opposite to the applied field/ appearing at given temperatures during warming, are of special interest. These currents, which are discussed in detail in [40, 41], were found to be very high in alcohols [38] /Fig. 13/. The negative currents can be attributed to the spontaneous ordering and reorientation of dipolar molecules taking place at given temperatures and resulting in the formation of electrets stable only in a given range of temperatures. Electret formation has been already observed in other polar systems [42].

Table 1

Number of free electrons released during warming of 3-methylpentane after gamma irradiation at 77°K

Number of the peaks	Q electrons cm <sup>-2</sup>	Dose eV g <sup>-1</sup>	volt cm <sup>-1</sup>	Ref.
1	4 x 10 <sup>10</sup>	1.6 x 10 <sup>18</sup>	3 x 10 <sup>3</sup>	70
1 2	3.14 x 10 <sup>9</sup> 5.65 x 10 <sup>10</sup>	6 x 10 <sup>18</sup>	1.8 x 10 <sup>3</sup>	71
1-4	5 x 10 <sup>10</sup>	6.2 x 10 <sup>18</sup>	3.2 x 10 <sup>4</sup>	41
1	6.74 x 10 <sup>7</sup>	1.5 x 10 <sup>13</sup>	1.78 x 10 <sup>4</sup>	71
1 1 1 1	1.30 x 10 <sup>8</sup> 3.15 x 10 <sup>9</sup> 4.12 x 10 <sup>9</sup> 5.85 x 10 <sup>9</sup>	7.0 x 10 <sup>13</sup> 6.0 x 10 <sup>14</sup> 1.2 x 10 <sup>15</sup> 3.0 x 10 <sup>15</sup>	1.78 x 10 <sup>4</sup>	71

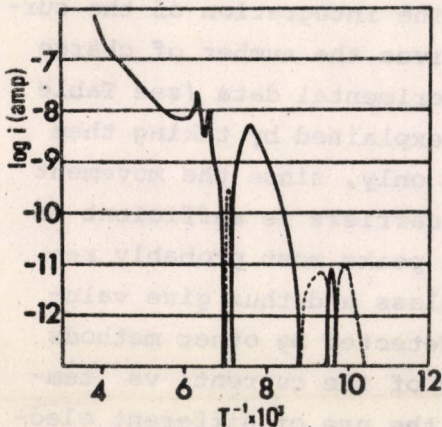


Fig. 13

Current vs sample temperature curve for ethanol gamma-irradiated with a dose of  $5.24 \times 10^{18}$  eV/g. Warming rate 2°C min<sup>-1</sup>. Dotted lines represent "negative" currents

The temperature profiles of the radiothermoluminescence /light intensity vs sample temperature/ curves are in a number of cases more or less similar to the current peaks measured during warming of the glass. However, there are current peaks without simultaneous increase in light emission, and vice-versa. The freeing of charge carriers and their re-trapping in deeper traps may produce current peaks not necessarily accompanied by light emission, while radical reactions can lead to luminescence without simultaneous current surge. The radiothermoluminescence method for structural investigations has lately been used successfully and thoroughly studied [43 - 47]. A simultaneous study of the temperature behaviour of

current and thermoluminescence during warming, combined with determination of the radiation quantum yield, could yield some information of interest on radiation reaction kinetics.

## 5. COMPILATION OF THE REPORTED DATA

The values of  $G_{fi}$  obtained from conductivity measurements are listed in Table 2 along with the values of the most important parameters of the formulae used for the calculations. The electrical conductivity is appreciably dependent on the purity of the sample. For information the minimum measured conductivity  $\sigma_n$  reported in the literature for different compounds are also listed. The very low conductivity observed in high-purity saturated hydrocarbons originates from the ionization brought about by cosmic radiation and radioactive material in the environment of the measuring cell. The minimum dark intrinsic conductivity of these hydrocarbons is thought, therefore, to lie between  $10^{-19}$ - $10^{-20}$  ohm $^{-1}$ cm $^{-1}$ . The natural conductivity, which is a measure of the purity of a material, is usually not specified by the authors. The minimum conductivity of alcohols and ethers, similarly to that of water, is determined by their dissociation [48]. The values of  $\sigma_n$  listed in the table have been calculated from the values of  $pK$  and the charge carrier mobility in the alcohols. Some data on the glassy phase are collected in the last row of the table.

## 6. CONCLUDING REMARKS

One of the frequently questioned problems in the conductivity of semiconductors and dielectrics is the mean free path of the charge carriers of low mobility. The average thermal energy of the free electrons in these substances, approximately  $kT$ , that is, not more than 0.03 eV. The wavelength  $\lambda = \sqrt{\frac{150.5}{V}} \left[ \frac{\text{\AA}}{\text{V}} \right]$  at this low energy is  $7 \cdot 10^{-7}$  cm. Taking the measured value  $\mu = 10^{-4}$  cm $^2$  volt $^{-1}$ sec $^{-1}$ , we get by the formula  $\mu = \frac{e\ell}{mv}$  ( $v \approx 10^{-7}$  cm/sec)  $\ell < \lambda$ , that is, the electron is formally reflected without any oscillation. This inequality is even more apparent if we consider the de Broglie equation  $\lambda = h/mv$  and the expression  $\ell = v\tau$ , which together give

$$v\tau > \frac{h}{mv}, \text{ that is, } mv^2 < \frac{h}{\tau}$$

It follows from the uncertainty relation that  $h/\tau = \Delta E$ . This implies that  $E < \Delta E$ , which means that the uncertainty of the electron energy is higher than its kinetic energy. We have to face the same difficulty in

Table 2

$G_{fi}$  values measured by electrical conductivity method and values of the parameters used in the calculations

Compound	$T$ K <sup>o</sup>	$\epsilon$	$10^5$ Poise	$\sigma_n$ ohm <sup>-1</sup> cm <sup>-1</sup>	$r_c$ $\frac{\Omega}{\lambda}$	$cm^2$ volt <sup>-1</sup> sec <sup>-1</sup> <sup>x</sup>		$G_{fi}^\sigma$	$G_{fi}^s$	Ref.	
						$\mu_+$	$\mu_-$				
n-butane	296		293 <sup>o</sup> 174			4±1 x10 <sup>2x</sup>				57	
n-pentane	293	1.84	239 227	2x10 <sup>-10</sup> 19,5°C	309	0.82	1.50	0.12		49	
	296	1.842			306			1.45		17	
	296						1.6±0.1x10 <sup>2</sup>				57
isopentane	296	1.838	293 <sup>o</sup> 224		307			0.170		17	
neopentane											
3.2-dimethylpropane	293	1.82	247		313	0.62	1.36	0.81		49	
neopentane	296	1.777			318			0.857		17	
	296					55±5x10 <sup>3</sup>				57	
2.2-dimethylpropane with 54 torr SiF <sub>6</sub>	293					0.52	1.38	0.47		49	
cyclopentane	296	1.960	293 <sup>o</sup> 439		288			0.155		17	
	296					1.1±0.1x10 <sup>3</sup>				57	
n-hexane	293	1.89	318	18 <sup>o</sup> 1x10 <sup>-18</sup>	302	0.64	1.11	0.11		49,3	
				4.5x10 <sup>-19</sup>							
	293	1.89	318	1.5x10 <sup>-18</sup>	302					50	
	296		329			0.15±0.05				51	
	296	1.885		8.3x10 <sup>-17</sup>	299			0.131		17	
		room					0.38	0.76			55
								1.30			
							0.41	0.92			55
cyclohexane	293					0.58	1.25				
							1.0			56	
	293		312			90±10				57	
	296					0.58	0.92			58	
	293	2.02	979 965		282	0.21	0.38	0.11		49	
	298	2.015			278,1				0.150		
	296	2.022 2.222			279 254			0.148 0.150		17	
	296					3,5±3x10 <sup>2</sup>				57	
neohexane											
2.2-dimethylbutane	293	1.87	375		305	0.48	0.97	0.40		49	
neohexane	296	1.926			293			0.304		17	
	296					10±1x10 <sup>3</sup>				57	
2.2-dimethylbutane with 1.0 torr SF <sub>6</sub>	293					0.36	0.96	0.20		49	
2.3-dimethylbutane	296	1.953			289			0.192		17	
hexene-1	296	2.046	260		276			0.062		17	
3-methylpentane	296	1.901		5x10 <sup>-18</sup>	297			0.146		17,41	
n-heptane	296		20°C 416 417	1x10 <sup>-13</sup>		2.4±0.5x10 <sup>4</sup>				51	
	293		409			0.42	0.66			58	
			20°C 541				3±1x10 <sup>-4</sup>				51
n-octane	296	1.94	546								
	296	1.944			290			0.124		17	
	290		560			0.28	0.51			58	

\* Mobility values placed in the middle of this column are for  $(\mu_+ + \mu_-)$

Compound	T K <sup>o</sup>	10 <sup>5</sup> Poise	n ohm <sup>-1</sup> cm <sup>-1</sup>	r <sub>o</sub> Å	10 <sup>3</sup> * cm <sup>2</sup> volt <sup>-1</sup> sec <sup>-1</sup>		G <sub>fi</sub> <sup>o</sup>	G <sub>fi</sub> <sup>s</sup>	Ref.
					μ <sub>+</sub>	μ <sub>-</sub>			
2.2.4-trimethylpentane	298	1.933	775					0.39	
	296	1.936			289.9		0.332		
	296					7±2x10 <sup>3</sup>			
n-nonane	290	1.97	714 740	1.7x10 <sup>-8</sup>	289	0.14	0.37		58
n-decane	296	1.98	22 <sup>o</sup> C 775 907		284	0.21±0.05			51
	290		1030			0.14	0.26		58
methanol	293		593						
ethanol	298	24.3	1096 1100	1.35x10 <sup>-9</sup>	23.6			1.01	18
n-butyl alcohol	298	17.1	2620		32.8			0.63	18
t-butyl alcohol	298	12.3	295.40 5588		45.6			0.67	18
n-pentyl alcohol	298	14.2			39.5			0.485	18
	337	10			49.6			0.46	18
neopentyl alcohol	337	8.3±0.3			59.7			0.21	18
n-butyl bromide	296±2	6.9			81		0.27		1
n-butyl chloride	296±2	7.2			78.4		0.39		1
diethyl ether	296±2	4.3	20 <sup>o</sup> C 244 122	25 <sup>o</sup> 4x10 <sup>-13</sup>	131.3		0.19		1
diethyl ether	296	4.280			132		0.350		17
n-buthyl ether	296±2	3.1			182.1		0.11		1
carbon disulfide	296	2.633		7.8x10 <sup>-18</sup>	214		0.314		17
carbon tetrachloride	296		21.2 <sup>o</sup> C 957	4x10 <sup>-18</sup>		0.40	0.33	0.068	11
	293	2.23	969			0.318	0.410		24
	296	2.232			253		0.096		17
1.4-dioxane	296	2.20		1x10 <sup>-19</sup>	255	0.80	0.48	0.038	11
	296	2.212			255		0.046		17
p-dioxane	296±2	2.2			256.6		0.45		1
germanium tetrachloride	296	2.435			232		0.127		17
nitromethane	298	37.8	262	18 <sup>o</sup> C 6x10 <sup>-7</sup>	14.82			0.31	18
tetramethylsilone	296					90±5x10 <sup>3</sup>			57
benzene	293	2.28	20 <sup>o</sup> C 649 647	7.6x10 <sup>-8</sup>		0.231	0.650		24
	298	2.294			244,3			0.055	18
	296	2.278			248		0.053		17
	293						0.45		56
	293.5		750			0.236	0.648		49
nitrobenzene	298	34.82	220	0 <sup>o</sup> C 5x10 <sup>-19</sup>	16.09			0.43	18
	r	34.82	220		16.09	0.062	0.035		62
toluene	298	2.379	590	1x10 <sup>-14</sup>	235.5			0.051	18
helium <sup>4</sup> He	0.9					52.0	37.2		59
nitrogen	77					0.9	10.6		60,61
helium at E=1.2 kV/cm	0.9						830		60
<sup>3</sup> He	3.4						900-400		63
3-methylpentane	77			< 10 <sup>-19</sup>					70
	77			~ 10 <sup>19</sup>					41
" " + TMPD	77			< 10 <sup>17</sup>		< 1.4			73
parafin /C <sub>25</sub> H <sub>52</sub> /	r			10 <sup>15</sup>					74
ethanol	77			< 10 <sup>13</sup>					38

\* Mobility values placed in the middle of this column are for /μ<sub>+</sub> + μ<sub>-</sub>/

the case of an electron thermalized in a liquid [64]. The free electron interacts with the surrounding molecules within a radius of  $\sim 70 \text{ \AA}$  at room temperature and a radius of  $\sim 150 \text{ \AA}$  at liquid  $N_2$  temperature. Thus the separation length is meaningful only after the trapping.

According to Freeman [4], the above argument can be objected to for two reasons. First, it is more appropriate to calculate the effective electron radius by using  $\lambda = \lambda/2\pi$  instead of  $\lambda$ ; second, in the calculation of  $\lambda$  one has to take into account the zero point energy of the localized thermalized electron, which is probably much greater than  $kT$ . If the latter is not more than 0.1 eV, we have  $\lambda = 6 \text{ \AA}$ , which is much lower than the above-mentioned  $70 \text{ \AA}$ .

This reduction of  $\lambda$  to  $6 \text{ \AA}$  does not solve the problem and it shows that although the theory describes well the conductance of metals it fails in the case of dielectric liquids and amorphous semiconductors. In these materials the mean free path of electrons is often smaller than the lattice spacing and sometimes even smaller than the interatomic distance. The probability of electron transition from one lattice site to another is low. If it does occur the electron has to surmount a barrier. The additional energy, the so-called activation energy, required for this is imparted to the electron by the thermal motion of the medium. The transition probability, and with it the mobility, vary proportionally to the Boltzmann factor, i.e.  $\mu \propto \exp -\frac{E}{kT}$ . Now, if  $\mu < 1 \text{ cm}^2/\text{volt sec}$  and this value increases with increasing temperature, the charge carriers eventually surmount the barrier and the electrical conduction is then governed by the mechanism known as hopping. In the intervals between jumps the electrons strongly interact with their environment; they are trapped. Thermal fluctuations may produce traps in pure substances; these are traps from where the ions or molecules drift apart. The trap concentration in liquids  $n_t \approx 10^{18} \text{ cm}^{-3}$ , and trap lifetimes vary between  $10^{-11}$  and  $10^{-12}$  sec. In amorphous material, e.g. glasses, these density fluctuations freeze in to permanent traps.

Recent investigations /e.g. [65-67]/ have shown that the zone theory can be applied to amorphous materials and even to liquids. The crystalline structure of solids and the long-range order are not prerequisites of semiconductor behaviour. The electrical properties of glasses and liquids can be qualitatively explained in terms of a short-range order determined by the character of the chemical bonds between neighbours. The study of the mechanism of electrical conduction in liquids and glasses seems to be important because it may yield interesting contributions to the generalisation of semiconductor theory and hence lead to the development of practically very useful equipments.

Still incompletely understood results are the values of  $\mu = 100 \text{ cm}^2/\text{volt sec}$  measured on hexane by Schmidt et al. [57] and Minday et al. [76]  $\mu = 0.1 \text{ cm}^2 \text{ volt}^{-1} \text{ sec}^{-1}$  using a pulse method. These values exceed other experimental values by 3-5 orders of magnitude. The electric conduction of very pure apolar systems can be regarded as analogous to that of liquefied noble gases, so that the mobility of the nonsolvated electrons which do not interact with any impurity can be similar to that of the electrons in noble gases  $\mu \approx 10^2 \text{ cm}^2/\text{volt sec}$ . Solvation, however, generally takes place in  $10^{-11} \text{ sec}$  and thus it is difficult to detect bare nonsolvated electrons by the present measuring techniques. Anyhow, it seems desirable to confirm these results by additional measurements.

The study of the electrical conductance in dielectrics irradiated with high energy radiations at high dose rates called attention to the difference in the temperature behaviour of the very low dark currents and the radiation-induced currents. The low dark currents probably reflect above all the contributions from electrode processes, and they are therefore expected to yield information on the structure of the junction and not on the electrical properties of the dielectric itself. At higher dose rates, when the concentration of the free charge carriers is very high, the nature of the transport processes is probably substantially changed by interactions between the carriers and between the carriers and the dielectric. This effect should be taken into account in the present high-power pulse conductivity measurements.

The increasing scientific and practical importance of amorphous semiconductors will probably stimulate in the coming years the study of their electrical properties and among them the radiation-induced conductivity of a large variety of such materials. The investigation of glassy and amorphous materials seems to be of particular interest because of their potential industrial use [67, 72]. These materials have been, as yet, hardly investigated and the available data are often contradictory. Radiation chemists have already contributed and will continue to contribute to the elucidation of many problems in this field.

#### ACKNOWLEDGEMENTS

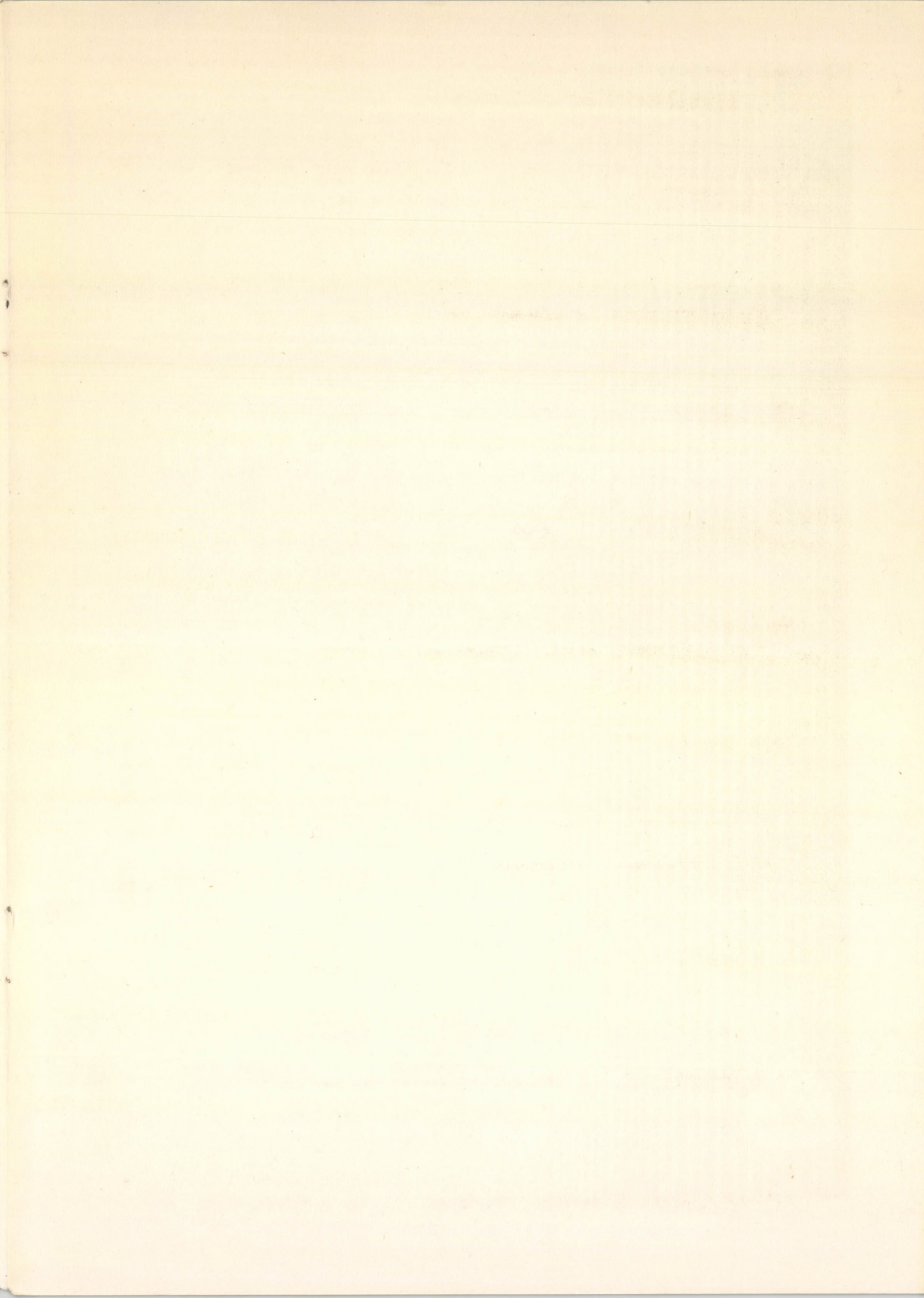
I would like to thank Mrs. Maria Gécs Erő, Gábor Jancsó and Timothy Wilkinson for reading the manuscript and for their helpful comments.

REFERENCES

- [1] G.R. Freeman and J.M. Fayadh, *J. Chem. Phys.*, 43, 86 /1965/
- [2] G.R. Freeman, *J. Chem. Phys.*, 39, 988 /1963/
- [3] I. Adamczewski, *Ionization, Conductivity and Breakdown in Dielectric Liquids*, Taylor & Francis Ltd., London 1969
- [4] G.R. Freeman, *Rad. Res. Rev.*, 1, 1 /1968/
- [5] D.W. Brazier and G.R. Freeman, *Canad. J. Chem.*, 47, 885 /1969/
- [6] W. Nowak, Doctorate Thesis, Technical University of Czczecin, Poland 1963, cited in [3]
- [7] I. Adamczewski, *Atompraxis* 9, 327 /1961/
- [8] L. Onsager, *Phys. Rev.*, 54, 554 /1938/
- [9] G.R. Freeman, *J. Chem. Phys.*, 46, 2822 /1967/
- [10] A. Hummel and A.O. Allen, *J. Chem. Phys.*, 44, 3426 /1966/
- [11] A. Hummel, A.O. Allen and F.H. Watson, Jr., *J. Chem. Phys.*, 44, 3431 /1966/
- [12] A. Mozumder and J.L. Magee, *J. Chem. Phys.*, 47, 939 /1967/
- [13] D.E. Lea, *Actions of Radiations on Living Cells*. Cambridge University Press, Cambridge, 1955
- [14] A. Mozumder and J.L. Magee, *Radiation Res.*, 28, 203-215 /1966/
- [15] A. Mozumder and J.L. Magee, *J. Chem. Phys.*, 45, 3332 /1966/
- [16] A. Mozumder, *Charged Particle Tracks and Their Structure in Advances in Radiation Chemistry*. Edited by M. Burton and J.L. Magee, Vol.1. Wiley-Interscience 1969
- [17] W.F. Schmidt and A.O. Allen, *J. Phys. Chem.*, 72, 3730 /1968/
- [18] C. Capellos and A.O. Allen, *J. Phys. Chem.*, 74, 840 /1970/
- [19] G.R. Freeman, *Radiation Chemistry II. Advances in Chemistry Series 82*, Washington, D.C. 1968
- [20] H.A. Bethe and J. Ashkin, in E. Segré, *Experimental Nuclear Physics Vol. 1.*, John Wiley and Sons, New York 1953
- [21] P.R.J. Burch, *Rad. Res.*, 6, 289 /1957/
- [22] J.F. Keithley, *Electrometer measurements*, Keithley Instruments
- [23] O.H. LeBlanc, *J. Chem. Phys.*, 30, 1443 /1959/
- [24] C. Lewa, *Acta Phys. Polon.*, 34, 165 /1968/
- [25] G. Kleinheins, *J. Phys. D: Appl. Phys.*, 3, 75 /1970/

- [26] V. Essex and P.E. Secker, *Brit. J. Appl. Phys.*, 1, 63 /1968/
- [27] D.E. Kearns and M. Calvin, *J. Chem. Phys.*, 34, 2022 /1961/
- [28] R.H. Bube, *Photoconductivity of Solids*, John Wiley et Sons, New York, London 1960
- [29] А.Ф. Иоффе, *Физика полупроводников*, Изд. АН СССР Москва-Ленинград 1957
- [30] Л.С. Стилбанс, *Физика полупроводников*, "Советское Радио", Москва 1967
- [31] E.B. Baker and H.A. Boltz, *Phys. Rev.*, 51, 275 /1937/
- [32] L.E. Lyons, *Physics and Chemistry of the organic solid state*, vol. 1. Intersci. Publ. New York-London 1963, p.745
- [33] Z. Croitoru, *Progress in Dielectrics*, 6, 103 /1965/
- [34] J. Dantscher, *Ann. Phys. Lpz.*, 5, 179 /1932/
- [35] Z. Croitoru, *Bull. Soc. Franc. Electr.*, 8, 342 /1960/
- [36] J.W. Boag, *Radiation Dosimetry*, Academic Press, New York-London, 1964. p. 70
- [37] E.C. Gregg and G. Bakale, *Rad. Res.*, 42, 13 /1970/
- [38] I. Kosa Somogyi, *Proc. 9th Japan Conf. on Radioisotopes*, Tokyo, 1969
- [39] J.T. Richards and J.K. Thomas, *J. Chem. Phys.*, 53, 218 /1970/
- [40] J.E. Willard, *Fundamental Processes in Radiation Chemistry*, John Wiley et Sons, 1968. p. 599
- [41] B. Wiseall and J.E. Willard, *J. Chem. Phys.*, 46, 4387 /1967/
- [42] F. Gutmann, *Rev. Mod. Phys.*, 20, 457 /1948/
- [43] N.Ya. Buben and V.G. Nikols'kii, *Proc. 3<sup>d</sup> International Cong. of Rad. Res.*, North Holland, 1967, p.288
- [44] Kh.S. Bagdassarian, R.I. Milutinskaya and Yu. V. Kovalev, *Proc. 3<sup>d</sup> Int. Cong. Rad. Res.*, North Holland, 1967, p.148
- [45] J. Bullot and A.C. Albrecht, *J. Chem. Phys.*, 51, 2220 /1969/
- [46] I. Kosa Somogyi, M. Gécs and M. Vizesy, *Proc. 2nd Tihany Symp. on Rad. Chem.*, Akadémiai Kiadó, Budapest 1967 p. 275
- [47] M.J. Capéran, J. Bullot, A. Dércoulède and F. Kieffer, *C.R. Acad. Sci. Paris*, 264, 1013 /1967/
- [48] G. Brière, *Thesis*, Masson et Cie Éditeurs, Paris 1963
- [49] P.H. Tewari and G.R. Freeman, *J. Chem. Phys.*, 49, 4394 /1968/
- [50] M. Chybicki, *Acta Phys. Polonica*, 34, 285 /1968/
- [51] V. Essex and P.E. Secker, *Brit. J. Appl. Phys.*, ser 2. vol. 2. 1107 /1969/
- [52] D.W. Swan, *Brit. J. Appl. Phys.*, 13, 208 /1962/
- [53] N.A. Lange, *Handbook of Chemistry 10th Edition McGraw-Hill 1967*

- [54] Справочник Химика, 2-ое изд. том I, Научно-техн. изд. хим. лит. 1962
- [55] A. Hummel and A.O. Allen, Discussion of Faraday Soc., 36, 95 /1963/
- [56] P. Chong and Y. Inushi, Technology Reports of the Osaka University, vol. 10, No. 414, Osaka 1960
- [57] W.F. Schmidt and A.O. Allen, J. Chem. Phys., 52, 4788 /1970/
- [58] Czowski O., Doctorate Thesis Techn. Univ. of Gdansk cited in 3
- [59] H.T. Davis, S.A. Rice and L. Mayer, J. Chem. Phys., 39, 947 /1962/
- [60] L. Bruschi and M. Santini, Rev. Sci. Instr., 41, 102 /1970/
- [61] L. Bruschi, G. Mazzi and M. Santini, Phys. Rev. Letters, 1970
- [62] G. Briere and F. Gaspard, Chem. Phys., Letter, 1, 707 /1968/
- [63] I. Modena and F.P. Ricci, Phys. Rev. Lett., 19, 347 /1967/
- [64] R. Schiller, J. Chem. Phys., 43, 2760 /1965/
- [65] А.И. Губанов, Квантово-электронная теория аморфных полупроводников, Изд. АН СССР, 1964.
- [66] A.F. Joffe and A.R. Regel, Non-Crystalline, Amorphous and Liquid Electronic Semiconductors, Progress in Semiconductors, vol. 4. Heywood and Co.Ltd., London 1960
- [67] M.H. Cohen, J. Non-Cryst. Solids. 4, 391 /1970/
- [68] P. Langevin, Ann. de Chim. et de Phys., 28, 433 /1903/
- [69] J.W. Boag, Ionization Dosimetry at High Intensities in Radiation Dosimetry. Academic Press New York and London 1964, p. 70
- [70] I. Kosa Somogyi and J. Balog, Advances in Chemistry Series, No. 82, Radiation Chemistry-II, Washington D.C. p.291
- [71] I. Kosa Somogyi, J. Balog and L. Tóth /to be published/
- [72] N.F. Mott, Advances in Phys., 16, 49 /1967/
- [73] H.S. Pilloff and A.C. Albrecht, J. Chem. Phys., 49, 4891 /1968/
- [74] Е.Л. Франкевич, Хим. Выс. Эн. I, 567 /1967/
- [75] R.M. Minday, L.D. Schmidt and H.T. Davis, J. Chem. Phys., 50, 1473 /1969/





Printed in the Central Research Institute for Physics  
Budapest, Hungary

Kiadja a KFKI Könyvtár és Kiadói Osztály  
O.v.: Dr. Farkas Istvánné  
Szakmai lektor: Jancsó Gábor  
Nyelvi lektor: Timothy Wilkinson  
Példányszám: 80 Munkaszám: 5417  
Készült a KFKI házi sokszorosítójában  
F.v.: Gyenes Imre  
Budapest, 1971. február 26.